C.P. No. 788

C.P. No. 788

MINISTRY OF AVIATION

AERONAUTICAL RESEARCH COUNCIL

CURRENT PAPERS

Effects of Varied Loading Paths on Fatigue Endurances

Part III - Some Stress Fatigue Properties of H46 at Elevated Temperatures

By

G.P. Tilly

LONDON: HER MAJESTY'S STATIONERY OFFICE

1965

EIGHT SHILLINGS NET

U.D.C. No. 539.431:536.49:669.15-194.57

C.P. No.788

June, 1964

Effects of varied loading paths on fatigue endurances PART III - Some stress fatigue properties of H46 at elevated temperatures

- by -

G. P. Tilly

SUMMARY

Constant stress amplitude fatigue tests have been carried out on an 11 per cent Cr-Mo-V-Nb steel (H46). The tests were conducted at 20°C, 400°C, 600°C and 700°C at 8000 c/m for push/pull and repeated tension loading, and at 6 c/m for repeated tension and were compared with available creep data of the same H46 forging. The resistance to static creep was greater than that to fatigue at 20°C and 400°C, but was less at 700°C. Similarly, the resistance to repeated tension fatigue at 8000 c/m was greater than that to 6 c/m fatigue at 700°C, but was less at 20°C.

Fatigue strain accumulated during the 6 c/m repeated tension tests according to laws similar to those that describe static creep strain behaviour. This was true at temperatures as low as 20°C provided the applied stresses were high enough. Static creep strain accumulated at a faster rate than fatigue strain at temperatures of 400°C and above. These differences were enhanced by an increase in temperature or stress.

The total secondary fatigue strain range (ε_T) appeared to be related to the number of cycles to failure (N) by an expression of the form $\varepsilon_T N^{\alpha}$ which was constant for a given temperature. The values of the exponent α varied according to the temperature.

Replaces N.G.T.E. Memo. No.M.387 - A.R.C.26 056

CONTENTS

TABLES

APPENDIX

ILLUSTRATIONS

1.0 Introduction

The tests described in this paper are part of a comprehensive programme[1] designed to produce a wide range of fatigue results that are applicable to gas turbine operating conditions. In the past, conventional fatigue tests have been made at frequencies of several thousands of cycles per minute and the material has been in a quasi-elastic condition because the loads were within the elastic region by virtue of the fact that the high loading rates raise the elastic limit of the material. This is not generally true of low frequency tests however, and the elastic limit is often exceeded during fatigue tests lasting less than 10^4 cycles to failure such as are relevant to gas turbine materials at elevated temperatures. Thus, there is a significant difference in the material response to the control of fatigue stress amplitude in a high frequency test as opposed to a low frequency test. In this investigation, low frequency constant stress amplitude fatigue tests were performed in a testing machine that was designed to compensate each fatigue loading, such that as the test-piece was deformed, the maximum stress per cycle was maintained constant.

The only known reported tests of low frequency, constant stress amplitude fatigue, were conducted by Landau[2,3] on an alloy of Nimonic 90 type at 800°C, 850°C and 900°C for repeated tension loading. He found that if the cumulative strain was plotted against time, the curve could be described by the same mathematical expression as that used in conventional constant stress creep. The particular expression that Landau used in the correlation was the Graham-Walles creep expression[4] which consists of a sum of power law components in terms of stress and time.

It appeared to be of interest to compare the low frequency constant stress amplitude fatigue data with high frequency data of the type produced by an Amsler Vibrophore test, since both tests may be considered to be similar by virtue of the fact that the high frequency tests are sensibly elastic and can be considered to be either constant stress, strain or load amplitude tests. In addition, the majority of fatigue data available in the literature is of the high frequency variety. Comparisons of tests conducted over a wide range of applied frequency both illustrate the effect of large variations in applied frequency on the life to failure, and assist the correlation of low frequency low endurance fatigue with conventional high frequency fatigue.

Some of the effects of variation in the applied frequency on constant load amplitude elevated temperature fatigue resistance of Nimonic 90 have already been considered[1]. It was shown that the life to failure at a given applied stress is determined by the number of fatigue repetitions at low temperatures, whereas it is determined by the total time of application at elevated temperatures. The dependence of such frequency effects upon the testing temperature was described by a frequency exponent m.

The form of fatigue loading in a gas turbine varies from one component to another. In the case of a turbine disc, a thermal fatigue cycle is imposed each time the component is heated and spun during a service operation. The most severe stresses occur close to the bore of the disc and at stress concentrations around the cooling holes, shaft fixing holes and fir tree blade fixings. The stress system is incurred by the centrifugal loading and comprises radial, tangential and hoop components. The nature of the fatigue repetition, considered overall, is close to constant

load amplitude fatigue, and the life to failure can be of the order of 10^4 cycles. Examination of turbine discs during service may under some circumstances, reveal the presence of cracks even after only a fraction of the expected life. In the case of turbine blades, thermal fatigue cycles are applied by the heating up and cooling down of the component resulting in compressive and tensile stresses at the blade edges. This is usually considered to be a form of fatigue closely comparable to constant strain amplitude fatigue at the upper temperature. This simple approach is becoming less tenable in view of the poor correlation with laboratory thermal shock test data on tapered disc specimens of Nimonic-type alloys[5]. Furthermore, tests on the thermal shock resistance (based on the first observed crack) of similar disc specimens with internal air cooling[6] apparently failed to give any correlation with the expression

$$\varepsilon_p N^k = \text{const} \qquad \ldots\ldots(1)$$

where

ε_p plastic strain range

N number of cycles to failure

k exponent

which has been successful in describing most constant strain amplitude tests[7]. However the data appear to be more closely explicable by recourse to the constant stress amplitude fatigue data produced by Landau[2]. Low frequency constant stress amplitude fatigue tests have the merit that they can be fairly simply analysed by the same techniques that have been successfully applied to creep data, and such data appear to be relevant to the fatigue conditions imposed on gas turbine components during service.

2.0 Experimental technique

The constant stress amplitude fatigue tests were performed in a 2 ton vertical lever arm type testing machine designed at N.G.T.E.[4]. Load was applied by a variable speed electric motor through a nine speed gear box and a pair of electro-magnetic clutches, to soft coil springs suspended from a 20/1 cranked lever arm. The reversal of loading direction at the maximum and minimum stress values was controlled by upper and lower micro-switches which could be preset within the travel of the coil springs. The micro-switches controlled a relay circuit such that one magnetic clutch was energised for loading, and the other for unloading. The maximum stress per cycle was maintained constant by the tilting of the cranked lever as the specimen deformed in a tensile sense. The minimum reversal stress was set at just greater than zero (at about 1.0 t.s.i.) in order to avoid slack in the system and subsequent loss of axial alignment of the specimen. The resulting reduction in the 20/1 leverage was designed to compensate the decrease in cross-sectional area of the specimen such that the ratio of maximum load over area remained constant. This was of course based on the assumption of uniform deformation and was ineffective for tests in which the specimen exhibited local deformation or necking.

The loading system was essentially 'soft' in the sense that the loading components of the machine were of very low elasticity and the rate

of release of stored energy by a fracture was small compared with that of a 'hard' machine. The stress/time cycle profiles were triangular (saw-toothed) in shape and there was zero dwell time at the maximum and minimum loads.

Heat was applied to the specimen by a Nichrome-wound electrical resistance furnace, 18 in. long and 3 in. internal diameter with separate upper, middle and lower windings. The voltages of the windings were controlled independently such that a uniform temperature distribution could be ensured. The temperature of the furnace was controlled by a high sensitivity saturable reactor type controller to better than $\pm\frac{1}{2}^{o}$C. Three thermocouples were tied to the specimen by asbestos string and continuous temperature records were made on a strip-chart recorder.

The load was measured by the elastic deformation of two copper/beryllium rods loaded in series with the specimen. A clock type dial gauge was mounted such that it recorded the deformation of these rods. The system was calibrated against a standard 2 ton proving ring, and operated to an accuracy of ±0.0005 ton.

Deformation of the specimen over a 1 in. gauge length was sensed by two differential transformer type transducers fitted to a pair of extensometers which were set up diametrically opposite one another on the specimen gauge length. Each extensometer consisted of a pair of arms clipped to upper and lower ridges which were machined on the specimens (see Figure 1) and maintained in place by leaf springs. Deformation of the specimen resulted in a relative longitudinal movement between the arms which could run freely on hardened steel roller bearings fitted between the moving surfaces. The response signals were fed from the transducers to an amplifier/recorder unit such that the summed deformation was continuously recorded on a strip-chart. The duplicate assembly had the merit that it could be used as a check for bending effects which would be revealed by differing responses from the two extensometers. It was possible to operate the transducers over any one of six scale ranges depending upon the amount of deformation to be recorded. The maximum deflections on the strip-chart for these ranges corresponded to deformations of 0.001 in., 0.005 in., 0.010 in., 0.050 in., 0.100 in., and 0.200 in. on the specimen, and the maximum sensitivity was $\pm 10^{-6}$ in.

The high frequency tests (8000 c/m) were performed in a 2 ton Amsler Vibrophore testing machine. The experimental technique has been described in detail previously[8].

2.1 Experimental programme

The low frequency (6 c/m) tests were performed in the constant stress amplitude testing machine at 20°C, 400°C, 600°C and 700°C under repeated tension loading.

High frequency (8000 c/m) tests were performed in the Amsler Vibrophore testing machine at the same four temperatures for equal and opposite push/pull, and for repeated tension loading.

The maximum applied stress levels were selected with a view to producing durations to failure up to 100 hours.

2.2 Material

The material was from a vacuum cast H46 steel supplied as a 13 in. diameter forging. Blanks of $\frac{5}{8}$ in. square section were slit out in a longitudinal direction and were heat treated at 1150°C for 30 min and air-cooled followed by 3 hr at 640°C and air-cooled to give a hardness of between 351 and 357 V.P.N.

The chemical analysis was as follows:-

Element	% Composition		
Carbon	0.18	to	0.20
Manganese	0.79		0.90
Silicon	0.28		0.30
Sulphur	0.016		0.019
Phosphorus	0.013		0.017
Nickel	0.78		0.88
Chromium	11.0		11.4
Vanadium	0.38		0.41
Niobium	0.24		0.30
Molybdenum	0.55		0.64
Boron	0.0035		0.0040
Iron		Balance	

2.3 Test-pieces

The low frequency constant stress amplitude tests were carried out on a test-piece specially designed for the testing machine (illustrated in Figure 1) with a 1 in. constant diameter gauge length and $\frac{1}{2}$ in. diameter threaded ends. Additional constant diameter (0.510 in.) portions were machined at either end of the test-piece to facilitate the axial alignment in the testing machine. The extensometer arms were fitted to ridges (designated as "Z" in Figure 1) at each end of the gauge length.

The Vibrophore high frequency tests employed waisted specimens having an 0.25 in. constant diameter gauge length, and threaded ends[8]. A variety of standard sizes was available to suit the test conditions. The room temperature tests were made on a test-piece with $\frac{3}{8}$ in. threaded ends and a cross-sectional area of $\frac{1}{65}$ sq inch. The elevated temperature tests were made on test-pieces with $\frac{1}{2}$ in. threaded ends and cross-sectional areas of either $\frac{1}{20}$ sq in. or $\frac{1}{30}$ sq in. depending upon the magnitude of the applied stress.

In all cases the test-pieces were rough turned and finish ground to an accuracy of 10 micro-inches.

3.0 Results

3.1 The 6 c/m constant stress amplitude test data

The 6 c/m constant stress amplitude rupture test data were plotted on a maximum applied stress/time to failure (S/t) diagram (Figure 3) as

frequency tests, and there was no common range to form a basis of comparison for the respective S/N curves. The room temperature data could be more meaningfully presented as S/N curves, but could not be compared with the elevated temperature data as easily as the S/t curves. The endurances ranged from the minimum possible value (corresponding to the $\frac{1}{2}$ cycle or ultimate tensile strength) to just greater than 100 hr to failure.

It was clear that with the exception of the 400°C tests, the experimental scatter was encouragingly low, and well defined mean curves were drawn through the U.T.S. and fatigue test points at each temperature. The shapes of these S/t curves were similar to those observed for Nimonic 90 i.e., showing increase in slope with increasing time to failure and with increasing temperature. There was no tendency for any of the curves to exhibit the characteristic sigmoidal fatigue type shape usually associated with cyclic testing. The S/t slope for the 400°C data was very low and the experimental scatter appeared to be higher than at either 20°C, 600°C or 700°C. No failures were recorded at times between 0.0063 hr (the U.T.S. duration) and 27.12 hr, despite the fact that several of the fatigue tests were conducted at stresses within the scatter range of the U.T.S. of the material.

The continuously recorded strain data were analysed and plotted as total accumulated strain against time (Figures 6 to 8), and as the averaged total secondary strain amplitude against the number of cycles to failure (Figure 9). The accumulated strain/time curves exhibited clearly defined primary, secondary and tertiary regions (see Figures 6 to 8), and appeared to be closely similar in shape to those of static creep. In addition, the accumulated fatigue strain was analysed by the Graham-Walles power law technique[4,9]. The degree of success of this creep type analysis was represented by the closeness of the fit of the continuous curves to the test points of Figures 7 and 8. Creep data[16] at 400°C, 600°C and 700°C obtained by Hawker Siddeley Engines Ltd. under M.O.A. contract KS/1/0128 on material from the same H46 forging were analysed and the mean ε/t curves (extrapolated in some cases) were plotted as broken lines in Figures 6 to 8. These curves were compared with the fatigue ε/t curves at equal maximum nominal stresses.

The total secondary strain range was plotted logarithmically against number of cycles to failure (Figure 9). Straight lines were drawn through the test points to give the best immediate fit, and were not deliberately associated with a particular slope such as (-0.5) extensively reported by Coffin[6] for constant strain amplitude fatigue data. In general, the total strain range to produce failure in a given number of cycles or time appeared to decrease with increasing temperature e.g., failure in 10 hr was produced by a test whose total strain range was ~0.6 per cent at 20°C, and by ~0.126 per cent at 700°C (see Table III).

3.2 The 8000 c/m push/pull and repeated tension fatigue tests

In the case of the 8000 c/m fatigue tests, only the maximum applied stress and the duration to fracture were recorded. The rupture data are illustrated in Figure 2 as curves of maximum applied stress against time to fracture for both push/pull and repeated tension. (In this notation a test at $\pm$ 30.0 ton/sq in. was plotted at the same apparent stress level as a test at $^{+30.0}_{0}$ ton/sq in.) The room temperature test results have been previously considered in some detail[10]. It appeared that the 20°C, 400°C and 600°C data could be described by single straight line log S/log t

relations, whereas the 700°C data exhibited an increase in slope at the lower stresses. In the case of the tests at 20°C the S/t lines were of lower slope than those at the higher temperatures, and few results were produced with durations between 1 hr and 100 hr to failure. In general, the S/t slopes appeared to increase with increase in temperatures and values for push/pull and repeated tension were similar at each temperature (see Figure 2 and Table III). There was a steady decrease in fatigue strength with increase in temperature for both push/pull and repeated tension as evinced by the 10 hr cross-plots in Figure 5. In addition, the resistance to repeated tension stresses was greater than that to push/pull over the whole range of test temperature. The resistance to static creep was greater than to either form of fatigue at 400°C but was appreciably less at 700°C. At 600°C however, the resistance to creep was greater than that to 8000 c/m push/pull fatigue, but was less than to 8000 c/m repeated tension fatigue (see Figure 5). There was no evidence that plastic deformation or creep accumulated in the manner of Figures 6 to 8 during the tests. It appeared that once the fatigue loading had been applied and adjusted, the tests remained elastic, and the specimen accumulated no permanent deformation during the subsequent life.

3.3 The 6 c/m and 8000 c/m repeated tension fatigue data

The rupture data for the repeated tension fatigue tests at 6 c/m and at 8000 c/m were plotted as S/t curves (Figure 4). The curves illustrate a changeover in strength between room temperature where the 8000 c/m strength was relatively low, and 700°C where the 8000 c/m strength was relatively high. The respective curves crossed over at ~0.1 hr at 400°C, the fatigue strength at 8000 c/m being greater than that at 6 c/m at durations of less than 0.1 hour. The two frequencies resulted in similar strengths at 600°C, with the 8000 c/m frequency as slightly the stronger condition.

The change in order of strength is also illustrated by the 10 hr cross-plot curves of Figure 5. The 10 hr fatigue strengths of the 6 c/m tests were greater than those of the 8000 c/m repeated tension tests at 20°C, 400°C and 600°C but was less at 700°C.

4.0 Discussion

4.1 Fatigue rupture test data

The general shape of the S/t curves for the two respective fatigue frequencies (6 c/m and 8000 c/m) illustrated in Figures 2 and 3, were very similar to the previously reported data[1] of Nimonic 90. The elevated temperature rupture curves were similar to those characterising conventional creep behaviour to the extent that they exhibited an increase in S/t slope with decrease in stress. A comparison of the repeated tension fatigue data at 6 c/m and at 8000 c/m (Figure 4) revealed an interesting reversal in strength between 20°C and 700°C i.e., the resistance of the material was greatest to the 6 c/m fatigue at 20°C whereas it was greatest to the higher frequency (8000 c/m) at 700°C. This reversal appears to be a manifestation of the change from cycle dependent behaviour at low temperatures to time dependent behaviour at high temperatures. It was of course, not surprising that the S/t curves were widely separated at 20°C and such rupture data are usually plotted on a cycle base (as S/N curves) rather than a time base. Increase in the applied stress increased the tendency to time dependence as evinced by the convergence of the respective S/t curves at 400°C - an increase in testing temperature also

increased the tendency to time dependence up to 600°C, at which temperature the lives were closely similar. The lives at 700°C did not appear to be wholly time dependent i.e., the higher frequency tests exhibited longer durations as measured by either time or cycles. The same effect was also evident in Nimonic 90.

4.2 Comparison of fatigue and creep rupture data

It is of interest to examine the relative fatigue strengths with respect to static creep data on a 10 hr cross-plot diagram (Figure 5). The 10 hr fatigue stresses at temperatures within the range of cycle dependence (400°C and below) were all less than those of static creep. The static creep strength was less than that at either frequency of repeated tension fatigue test at 600°C, and less than that of push/pull as well as repeated tension at 700°C. In addition, the 8000 c/m push/pull strength and the 6 c/m repeated tension strength were similar at 700°C. This high temperature type behaviour has also been observed in Nimonic 90, and can be explained on the basis that the resistance of the material to creep is so poor under these conditions that the time spent in the tensile half of the fatigue cycle becomes of premier importance. The addition of a compressive half to the cycle has the effect of allowing the material a respite from the tensile creep, and can result in enhanced endurances at high temperatures (900°C in the case of Nimonic 90). It is possible that the higher frequency repeated tension fatigue (8000 c/m) results in a similar effect by virtue of the fact that the speed of application of the tensile loading raises the elastic limit to above the 10 hr stress, and reduces the severity of time dependent creep effects. The statement that the criterion of fatigue failure changes from one based on the number of repetitions of load (cycle dependent) at low temperatures to one based on the duration of stressing (time dependent) at high temperatures appears to be generally true for both forms of loading. There are however certain loading conditions such as the push/pull, and high frequency applications, that can modify the creep type behaviour such that an increase in applied frequency can result in an increase in both cycles and time to failure.

4.3 Fatigue and creep strain accumulation

The fatigue strain during the 6 c/m repeated tension tests appeared to accumulate according to similar laws that describe static creep behaviour. The general creep type behaviour in which the strain/time accumulation under repeated stresses is composed of primary, secondary and tertiary stages has been reported for such materials as Vitallium and Aluminium[11,12] at elevated temperatures, and has been termed 'dynamic creep'. The creep type behaviour of copper, aluminium and mild steel subjected to repeated tension load fatigue at room temperature has been termed 'cyclic creep'[13,14]. A more detailed examination of fatigue strain accumulation[2,3] was made on Nimonic 90 data at 800°C, 850°C and 900°C, and it was concluded that the strain/time accumulation could be described by an expression composed of a sum of power law components originally proposed by Andrade to describe static creep and incorporated in a more comprehensive formula by Graham[9].

$$\varepsilon = \sum C\sigma^{\beta}t^{\kappa} \qquad \ldots\ldots(2)$$

This expression has been invoked to describe the cumulative strains at 20°C, 400°C, 600°C and 700°C. The degree of success obtained by the theoretical expression is illustrated by the closeness of fit of the continuous curves to the test points in Figures 7 and 8.

The strain data obtained at 20°C are significant because they demonstrate that creep type accumulation of strain can take place at such temperatures provided that the maximum applied fatigue stress is high enough. Similar effects have also been reported[15] for copper at a temperature as low as -196°C. A static load creep test at 71.5 t.s.i. and 20°C produced primary and secondary stages, and though still creeping after 22 hr at a similar creep rate to the fatigue tests at equivalent maximum stresses, did not have as high a total strain and did not exhibit tertiary deformation. The tertiary regime that is invoked by the cyclic loading at 20°C is possibly a manifestation of work softening, since it is at the stage that the stress/strain hysteresis loops widen out and increase in area. (A typical example of work softening at an elevated temperature is illustrated in Figure 10.2.) The inference that the mathematical description remains the same for the tertiary stage of a static creep curve as that for the tertiary stage of a high stress room temperature fatigue test, appears to be most important because it is an added verification that a time dependent failure mechanism is operative. Furthermore, it is a useful extension of the experimental range over which a general creep type descriptor can be applied.

All the 6 c/m fatigue tests at 400°C exceeded 27 hr duration and the strain/time records exhibited little tertiary creep deformation. This was contrary to the deformation behaviour at room temperature and appeared to be associated with strain ageing effects which were shown to be operative at 400°C. Comparison with typical static creep records (from Reference 16) of tests at ~53.2, 54.7 and 57.5 t.s.i. revealed that the static loading produced continuous deformation into tertiary creep at a much faster rate than did the fatigue tests. It appeared that the material strain aged markedly at 400°C under the fatigue loading conditions that were applied, and the deformation was mostly confined to the setting up first half cycle. Little additional deformation occurred during subsequent cycles and the material was effectively 'hardened', whereas it deformed continuously under a continuous static creep load. (A test is illustrated in Figure 10.1 in which the first load reversal was at 57.5 t.s.i., followed by a second reversal at 58.1 t.s.i. - the second loading was all-elastic despite the fact that it had not been previously plastically deformed beyond 57.5 t.s.i.) Metallographic examination at magnification of × 750 of creep tested material at 20°C, 400°C, 600°C and 700°C revealed that carbides had precipitated out on grain boundaries at 400°C and above, but there was no obvious metallurgical correlation with the strain ageing behaviour[16].

The elevated temperature fatigue strains at 400°C, 600°C and 700°C exhibited well defined tertiary regimes and were very closely fitted by the theoretical creep curves (Figures 7 and 8). The static creep curves exhibited similar shapes to the fatigue curves but generally accumulated strain at a faster rate than in the fatigue tests and rupture occurred at shorter durations. The separation of the static and fatigue curves at

decrease at high temperatures. This has also been observed on close packed metals and was suggested as an alternative definition of cycle or time dependent behaviour[15].

It is clear from data such as that illustrated in Figure 7 that the times endured at high stresses are more detrimental to life at the elevated temperatures than are the number of repetitions. The unloading half of a fatigue cycle can either allow the material strain ageing to become effective (as at 400°C), or else it can simply interrupt the creep operation and slow it down. High stress cycles at 20°C did not appear to markedly strain age the material, but resulted in an enhanced creep accumulation.

Data expressed on log/log graphs of total secondary strain range (ε_T) against number of cycles to failure (N) for 6 c/m repeated tension fatigue were closely fitted by straight lines at each temperature (Figure 9). The general form of the power law expression which describes this fit can be expressed as

$$\varepsilon_T N^{\alpha} = c \qquad \ldots\ldots(3)$$

where the numerical values of the constants α and c are dependent upon the temperature. Values of the total secondary strain to produce failure in 10 hr duration were calculated from Figure 9 and recorded in Table III. It was clear that this 10 hr strain range decreased with increase in temperature at a similar rate to the 10 hr stress in Figure 5 (see Table III).

4.4 The elastic and plastic fatigue strain components

In general, ε_T may be expressed as the sum of the plastic (ε_p) and the elastic (ε_E) components

$$\varepsilon_T = \varepsilon_p + \varepsilon_E \qquad \ldots\ldots(4)$$

But, the total accumulated strain (ε) has been shown above to be described by a sum of power law components expressed by Equation (2). The general expression may be considered for the case of a single component only and becomes

$$\varepsilon = \sigma^{\beta} t^{\kappa} \qquad \ldots\ldots(5)$$

If it is assumed that the plastic strain recovery during the unloading half of a cycle is negligibly small compared with the plastic strain accumulation during cyclic loading, the plastic strain range (ε_p) may be defined as the difference between the total strain at (n + 1) cycles and at n cycles.

$$\varepsilon_p = \varepsilon_{n+1} - \varepsilon_n$$

$$\varepsilon_p = C\sigma^\beta \left[\left(\frac{n+1}{f} \right)^\kappa - \left(\frac{n}{f} \right)^\kappa \right]$$

$$\varepsilon_p = \frac{C\sigma^\beta}{f^\kappa} \left(n + 1 \right)^{\kappa - 1} \qquad \ldots\ldots(6)$$

and Equation (3) becomes

$$\left[\frac{C\sigma^\beta}{f^\kappa} \left(n + 1 \right)^{\kappa - 1} + \frac{\sigma}{E} \right] N^\alpha = \text{constant}$$

and for the special case of total strain range evaluated from data of the secondary fatigue strain region where it is usually considered that $\kappa = 1$, Equation (3) becomes

$$\frac{C\sigma^\beta}{f} N^\alpha + \frac{\sigma}{E} N^\alpha = A \qquad \ldots\ldots(7)$$

where A = constant

This expression is of course operative for low cycle fatigue only and no corrections have been made to account for the presence of a fatigue limit - the usual practice is to express the number of cycles as $(n - n_0)$ and the stress as $(\sigma - \sigma_0)$ where n_0 and σ_0 are the fatigue limit duration and stress respectively. Several assumptions were made to enable approximate values of the constants to be calculated for 20°C, 600°C and 700°C and lives were calculated at each temperature, and compared back with the experimental values (see Appendix).

The plastic strain component in Equation (7) appears to be the chief factor determining time dependent failure since it becomes dominant at high stresses and temperatures, where time dependence has been shown to be operative. On the same reasoning, the elastic component is probably the dominating factor determining cycle dependent failure at low temperatures and stresses.

The effect of change in applied frequency is to modify the plastic strain component only and to leave the apparent elastic component unchanged. A decrease in applied frequency results in an increase in ε_p, and the number of cycles to failure is increased. An increase in frequency suppresses the plastic component and if the frequency is made high enough the strain may become effectively all-elastic such that Equation (7) becomes

$$\sigma n^\alpha = \text{const} \qquad \ldots\ldots(8)$$

Thus, in the case of the high frequency (all-elastic) fatigue tests, the slope of the log stress/log duration curve is given by α, whilst low frequency tests exhibiting plastic strain have log ε_T/log N curves of slope α. The value of α appears to vary with frequency and stress as well as with temperature. A similar power relation between applied stress and number of cycles to failure has been used successfully for other materials and such a relation formed the basis of the Harris formula[17]. A similar expression has also been shown by Manson[18] to apply to constant strain amplitude fatigue data of a large range of materials for which a universal value of α = 0.12 was proposed. The data in Figure 2 could be fitted by an expression of this form although the scatter of the 8000 c/m test data was higher than that at 6 c/m, and values of α could not be established with certainty. The 6 c/m test data was more amenable to analysis. The values of α calculated from the slopes of the curves in Figure 9 varied between α = 0.057 at 20°C and α = 0.220 at 400°C (see Table III) though the interpretation of the 400°C data is debatable since it exhibited greater scatter than that at the other temperatures. There was no clearly defined relation between α and temperature for the temperature range of the tests, and this appears to be a feature worthy of further investigation at other temperatures and frequencies.

The case of low frequency fatigue where there is appreciable plastic deformation, described by the full form of Equation (7), has been considered by Benham[14] for mild steel and an aluminium alloy. Evidence was produced that suggested that the total secondary strain range during a constant load amplitude fatigue test predicted the same rupture lives as did that of a constant strain amplitude test. This is a conclusion that appears intuitively to be correct, and has been assumed subsequently in an analysis of Nimonic 90 data[19]. If this is true, then Equation (7) is itself a universal descriptor which can be related to the well known Coffin expression (Equation (1)) in which the exponent was 0.5 for a wide range of experimental conditions.

5.0 Conclusions

(i) The H46 material was less resistant in terms of time to failure, to the higher frequency (8000 c/m) repeated tension fatigue than to the 6 c/m fatigue at 20°C, whereas it was more resistant to the 8000 c/m fatigue at 700°C.

(ii) The resistance to static creep was greater than to fatigue up to 400°C. There was an inversion in behaviour at around 600°C, and the material was less resistant to static creep than to fatigue at 700°C.

(iii) The strain during the repeated tension fatigue tests at 6 c/m accumulated according to laws similar to those that describe static creep strain.

(v) Creep type strain accumulation could be induced during fatigue tests at temperatures as low as 20°C, provided that the applied fatigue stress was high enough.

(vi) Static creep strains at 400°C, 600°C and 700°C accumulated at a faster rate than did the fatigue strains at equal maximum applied stresses. These differences became more marked at increased stresses.

(vii) The total secondary fatigue strain range appeared to be related to the number of cycles to failure (or time) by an equation of the form

$$\varepsilon_T N^{\alpha} = \text{const}$$

where the values of the exponent α varied according to temperature.

ACKNOWLEDGEMENTS

The author gratefully acknowledges many helpful discussions with Mr. A. Graham, and his permission to test the H46 pedigree steel. The assistance of Mr. W. Gwenlan who set up the Vibrophore tests, and Mr. G. J. Bates who supervised the heat treatment and hardness testing of the material is also acknowledged.

NOTATION

U.T.S.	ultimate tensile strength expressed in ton/in^2
V.P.N.	Vickers pyramid hardness number
σ	applied stress
S	maximum applied stress/cycle
n	number of cycles
N	number of cycles to failure
t	time in hours
f	applied frequency
E	Young's modulus of elasticity
ε	strain
ε_T	total secondary strain range
ε_E	elastic strain range
ε_p	plastic strain range
α	total strain range exponent
k	plastic strain range exponent
β	stress exponent
κ	time exponent
m	frequency exponent
b	constant for a given stress
A, C, c	material constants

REFERENCES

No.	Author(s)	Title, etc.
1	G. P. Tilly	Effects of varied loading paths on fatigue endurances Part I - Some load fatigue properties of Nimonic 90 at elevated temperatures. A.R.C. C.P.786. December 1963
2	C. S. Landau	Low frequency fatigue of Nimonic 90. N.G.T.E. Report No. R.243 September 1960 A.R.C.22 309
3	C. S. Landau	Low frequency fatigue - a rheological approach. The Engineer Vol. 214, 1962 p.911
4	K. F. A. Walles A. Graham	Unpublished M.O.A. Report.
5	P. G. Forrest K. Armstrong	The thermal fatigue resistance of Ni-Cr alloys. Joint A.S.M.E. - Inst. Mech E. International Creep Conference October 1963
6	J. T. Roberts	Comparative thermal fatigue test on Nimonic 90 tapered disc specimens with and without internal air cooling. A.R.C.25 322. September, 1963
7	L. F. Coffin	Trans. A.S.M.E. 1954, 76,931
8	N. Stephenson J. E. Northwood R. S. Smith	The effect of alternating stresses at elevated temperatures on structural changes in Nimonic 90. N.G.T.E. Memorandum No. M.325 July 1959
9.	A. Graham	The phenomenological method in rheology. Research (6) p.62, 1953
10	G. P. Tilly	Effects of varied loading paths on fatigue endurances Part II - Some load fatigue properties of H46 at room temperature. A.R.C. C.P.787. March 1964.
11	B. J. Lazan E. Westberg	Effect of tensile and compressive fatigue stress on creep, rupture and ductility properties of temperature resistant materials. Proc. A.S.T.M. Vol. 52 1952 p.837

REFERENCES (cont'd)

No.	Author(s)	Title, etc.
12	F. W. De Money B, J. Lazan	Dynamic creep and rupture properties of an aluminium alloy under axial static and fatigue stress. Proc. A.S.T.M. Vol. 54 1954 p.769
13	P. P. Benham	Axial - load and strain - cycling fatigue of copper at low endurance. J. of Inst. of Metals 1961 p.328
14	P. P. Benham H. Ford	Low endurance fatigue of mild steel and an aluminium alloy. J. of Mech. Eng. Sci. Vol. 3 No. 2 1961 p.119
15	C. E. Feltner G. M. Sinclair	Cyclic strain induced creep of close packed metals. Joint A.S.M.E. - Inst. Mech. E. International Creep Conference October 1963
16	W. J. Harris	Some observations of the static tensile and creep properties of the 11 per cent Cr-Mo-V-Nb steel H46. De Havilland Central Laboratory Report No. R250/51/63 M.O.A. Contract Number KS/1/0128
17	W. J. Harris	Metallic fatigue. Pergamon Press 1961
18	S. S. Manson	Thermal stresses in design - Part 19: Cyclic life of ductile materials. Machine Design Vol. 32 7th July, 1960 p.139
19	P. W. H. Howe	Unpublished M.O.A. Report
20	J. F. Eckel	The influence of frequency on the repeated bending life of acid lead. Proc. A.S.T.M. 51, 1951, p.745

TABLE I

Repeated tension fatigue tests at ~6 c/m

Temperature °C	Maximum applied stress (ton/in^2)	Cycles to failure	Life (hr)	%ε_T
20	72.0	½	0.0093	
	72.0	598	8.63	0.540
	71.5	6	0.09	0.790
	71.7	5	0.07	0.950
	70.5	2444	34.92	0.560
	70.3	2386	36.08	0.590
	71.4	919	14.5	0.590
	66.0	3587	54.9	-
	* 67.0	2031	140.5	0.467
	* 71.0	528	40.1	0.545
	* 70.5	2½	0.2	-
	* 69.5	11	1.3	-
	* 68.9	40	4.0	0.635
	* 66.6	112	10.6	0.575
	* 69.5	1½	0.15	-
400	45.5	8187	89.42	0.314 ϕ
	50.3	6127	76.94	0.348
	53.2	3320	47.41	0.373
	54.7	2148	30.49	0.414
	56.5	½	0.0067	
	57.3	2544	35.1	0.433
	56.4	4397	74.37	0.382
	55.8	½	0.0063	4.34
	54.3	½	0.0065	3.44
	54.8	2398	27.12	0.316
	57.5	2414	29.64	0.419
	52.5	2740	32.46	0.381
	51.0	3181	36.20	0.356
600	28.0	29366	205.5	0.249
	29.5	16060	119.4	0.274
	35.05	173	1.38	0.334
	32.7	2298	15.46	0.299
	39.3	½	0.0075	5.41
	37.2	21	0.28	
	31.65	2066	25.46	0.279
700	18.0	76	0.34	-
	16.7	1641	2.33	-
	15.55	2889	9.31	-
	14.4	2200	6.79	-
	13.0	1484	3.83	-
	12.0	6320	17.98	-
	10.5	60845	130.84	-
	23.4	½	0.0059	
	18.7	118	0.71	0.217

TABLE II

Repeated tension and push/pull fatigue tests at 8000 c/m

Temperatures °C	Repeated tension			Push/pull		
	Maximum applied stress (ton/in^2)	Cycles to failure	Life (hr)	Maximum applied stress (ton/in^2)	Cycles to failure	Life (hr)
20	69.3	10×10^3	0.021	47.6	13×10^3	0.0001
	68.0	12×10^3	0.025	45.0	95×10^3	0.166
	65.3	38×10^3	0.078	41.3	495×10^3	1.1
	61.3	815×10^3	1.7	41.3	162×10^3	0.35
	58.9	342×10^3	0.8	38.6	49050×10^3	107.6
	57.2	63118×10^3	113.1			
400	60.5	250	0.033	30.7	54×10^3	0.1
	55.8	875	0.111	29.8	1324×10^3	2.95
	51.0	230×10^3	0.5	26.4	28141×10^3	63.0
	47.9	1332×10^3	3.0	26.5	338×10^3	0.75
	44.9	512×10^3	1.15	26.6	94192×10^3	9.3
	41.9	8309×10^3	18.7	23.1	62801×10^3	137.7
				25.1	185×10^3	0.4
				25.2	40629×10^3	77.6
600	29.9	9779×10^3	22.05	20.0	431×10^3	1.0
	27.6	20450×10^3	56.3	17.0	3213×10^3	7.5
	34.7	479×10^3	1.1	13.95	47308×10^3	74.65
	32.5	2122×10^3	4.1	17.4	32783×10^3	64.9
				18.5	7046×10^3	14.1
				16.6	5252×10^3	10.0
				15.0	44778×10^3	84.3
				19.1	1341×10^3	2.55
				18.5	2392×10^3	6.45
700	15.15	59806×10^3	134.5	14.3	335×10^3	0.7
	16.9	10578×10^3	19.5	13.2	1029×10^3	2.3
	18.0	4047×10^3	8.3	11.9	8279×10^3	18.8
	19.8	3760×10^3	7.6	11.0	9584×10^3	19.3
	20.9	56×10^3	0.13	9.6	10316×10^3	20.9
	20.4	130×10^3	0.3	9.55	15013×10^3	28.7
	19.1	2800×10^3	5.4	16.1	50×10^3	0.13
				7.7	22993×10^3	45.8

TABLE III

Values of the 10 hr parameters and the strain exponents for fatigue at elevated temperatures

	Temperature °C			
	20	400	600	700
Fatigue parameters to produce 10 hr duration				
Repeated tension fatigue stress at 6 c/m(ton/in^2)	71.5	54.5	33.0	12.9
Repeated tension fatigue stress at 8000 c/m (ton/in^2)	58.5	43.5	30.5	17.7
Push/pull fatigue stress at 8000 c/m (ton/in^2)	40.0	26.5	17.0	11.5
Total cyclic strain range for 6 c/m repeated tension (%ε_T)	0.600	0.490	0.300	0.126
Static creep stress (ton/in^2)	>71.5*	55.5	25.5	9.5
Ratio of 10 hr repeated tension stress at 6 c/m to ε_T (ton/in^2)	11900	11100	11000	10200
Ratio of 10 hr repeated tension stress at 8000 c/m to ε_T (ton/in^2)	9750	8900	10200	14000
Exponent α for 6 c/m repeated tension	0.057	0.220	0.059	0.140
$1/\alpha$	17.6	4.55	17.0	7.15
Slope of 8000 c/m repeated tension S/t curve	1/43.5	1/17.5	1/19.3	† -
Slope of 8000 c/m push/pull S/t curve	1/45	1/16	1/13.1	† -

*A static load creep test at 71.5 ton/in^2 and 20°C was unbroken and still straining after 22 hr at which time it had accumulated 6.44 per cent strain.

†The 8000 c/m S/t data at 700°C could not be described adequately by a single power law component.

APPENDIX I

The evaluation of some of the fatigue and creep parameters

It has been shown experimentally that under certain conditions the number of cycles to failure of a slow repeated tension fatigue test may be related to the total secondary strain range by a power law expression of the form

$$\varepsilon_T N^{\alpha} = c \qquad \ldots\ldots(3)$$

and Equation (3) has been expanded into the general form

$$\frac{C\sigma^{\beta}}{f} N^{\alpha} + \frac{\sigma}{E} N^{\alpha} = A \qquad \ldots\ldots(7)$$

Equation (7) appears to be a promising expression for predicting fatigue lives from a small number of experiments, since it possesses the merit that it has elastic and plastic components, and can therefore be related to both fatigue and creep. It is true for only a limited range of frequency however, since it assumes that the total secondary strain range determines the number of cycles to failure independent of applied frequency. This assumption is not strictly true and subsequent experiments have demonstrated that the failure duration can be markedly affected by applied frequency. Data from Nimonic 90 has suggested that the frequency dependence of constant load amplitude fatigue at elevated temperatures may be described by a frequency exponent m given by the expression[1]

$$tf^{m} = b \qquad \ldots\ldots(9)$$

m = frequency exponent

b = a function of stress

subsequent data has suggested that although Equation (9) is true for a variety of conditions such as the low frequency fatigue of acid lead for which it was originally proposed[20], it is not strictly true for H46 and should be regarded as being descriptive of the behaviour of a perfect material rather than of an engineering material. Moreover, it is possible that the range of application should be limited to the low frequencies for which the equation was originally proposed. Nevertheless, it appears to form the basis of a reasonable first approximation to describe the frequency affect and generalise Equation (7) by substituting b in place of N

$$\frac{C\sigma^{\beta}}{f} b^{\alpha} + \frac{\sigma}{E} b^{\alpha} = A \qquad \ldots\ldots(11)$$

For the case of low temperature behaviour where the number of cycles to failure is independent of applied frequency, and m = 1, the abbreviated expression Equation (3) becomes $\varepsilon_T N^{\alpha}$, and for the case of high temperature behaviour where time to failure is independent of applied frequency, and m = 0, the expression becomes $\varepsilon_T t^{\alpha}$.

Values of m were evaluated at the maximum 100 hr stress values for 20°C, 600°C and 700°C and values of A and C were calculated at 20°C, 600°C and 700°C for the convenient values of $\kappa = 1$ and $\beta = 4$ selected from inspection of the creep data. (The data at 400°C was too scattered to enable meaningful values of the constants to be evaluated.)

Temperature °C	m	A	C
20	1.0	$7.85\ 10^{-3}$	$3.94\ 10^{-10}$
600	0.19	$3.61\ 10^{-3}$	$1.73\ 10^{-10}$
700	-0.2	$1.79\ 10^{-3}$	$1.24\ 10^{-8}$

These values of m, A and C may be used to predict lives to failure for either the 6 c/m or the 8000 c/m repeated tension fatigue tests.

Temperature °C	Maximum applied stress (ton/in²)	Predicted life at 6 c/m (hr)	Predicted life at 8000 c/m (hr)
20	72	16.6 (10)*	-
	69	52.5 (80)	-
	65	-	2.75 (0.1)
	60	-	10.2 (4)
	55	-	52.3 (180)
600	36	0.87 (1)	-
	33	5.5 (10)	1.95 (2.3)
	27	208 (400)	58.7 (80)
700	18	-	3.8 (12)
	16	1.06 (1.6)	8.85 (70)
	10	51.6 (65)	-
	8	273 (300)	-

*Figures in brackets are the experimental lives as defined by the mean S/t curves

The predicted lives were encouragingly close to the experimental points, and the equation appears to be capable of predicting lives within the range of conditions applied, but requires further attention to enlarge its scope. In particular, the usefulness of the equation would be improved by:-

(i) The use of a more comprehensive expression than the frequency exponent m to describe the frequency dependence.

(ii) A more detailed analysis of the contribution by cumulative creep such that values of κ and β of other than 1 and 4 could be incorporated.

(iii) The introduction of a stress/temperature parameter.

FIG.1

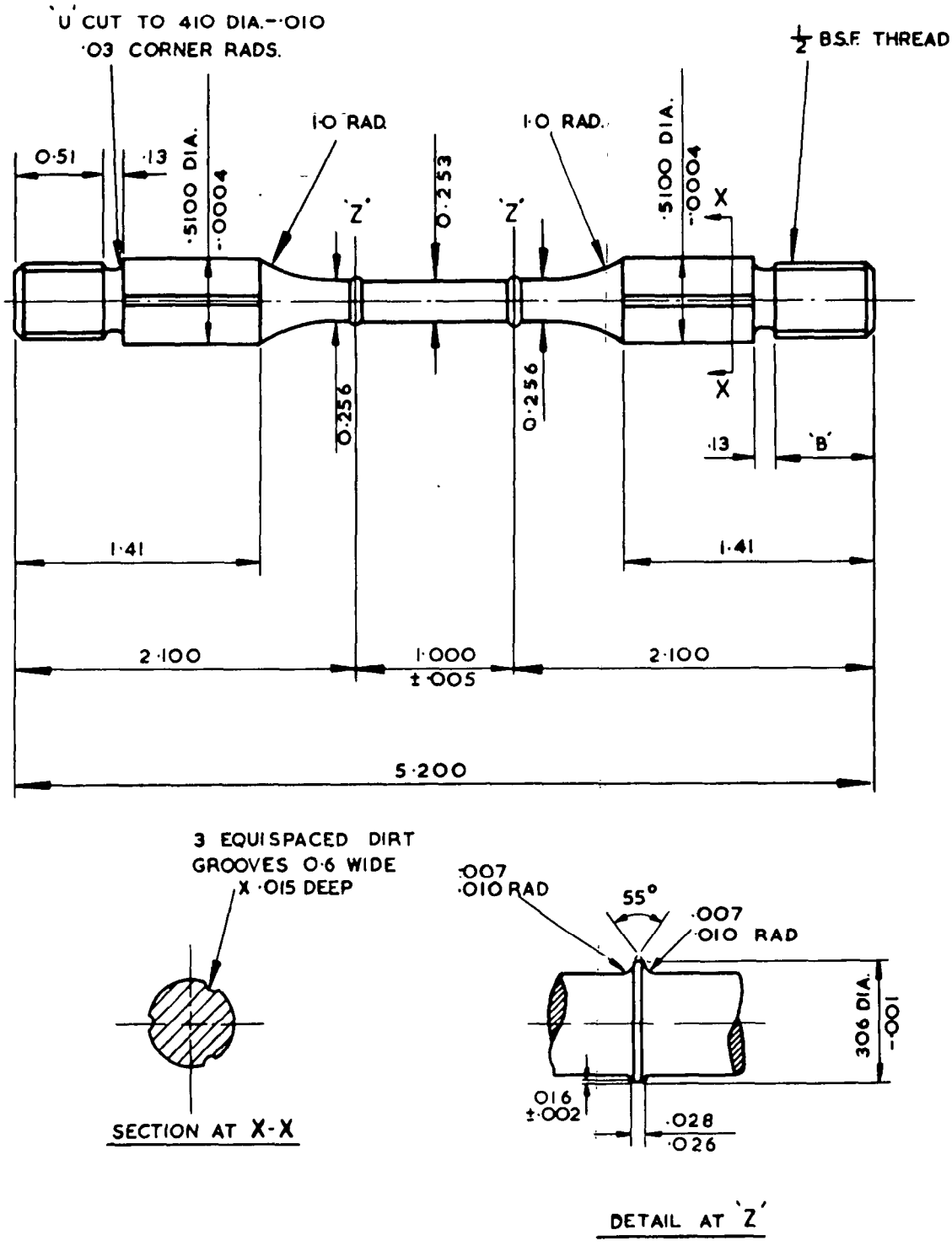

CONSTANT STRESS AMPLITUDE FATIGUE TEST-PIECE

FIG 2

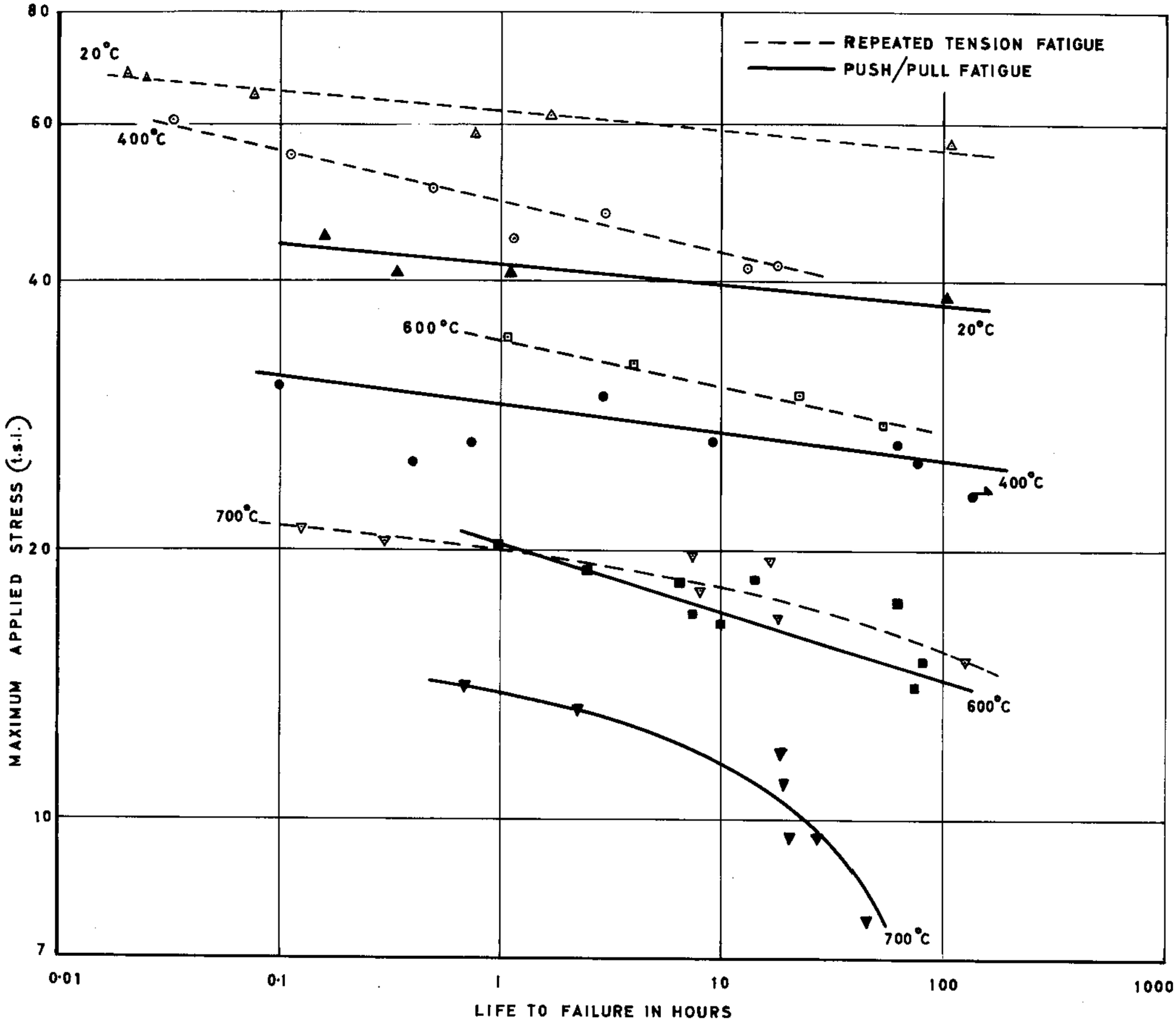

STRESS/TIME FATIGUE RUPTURE CURVES AT 8000 C/M

FIG. 3

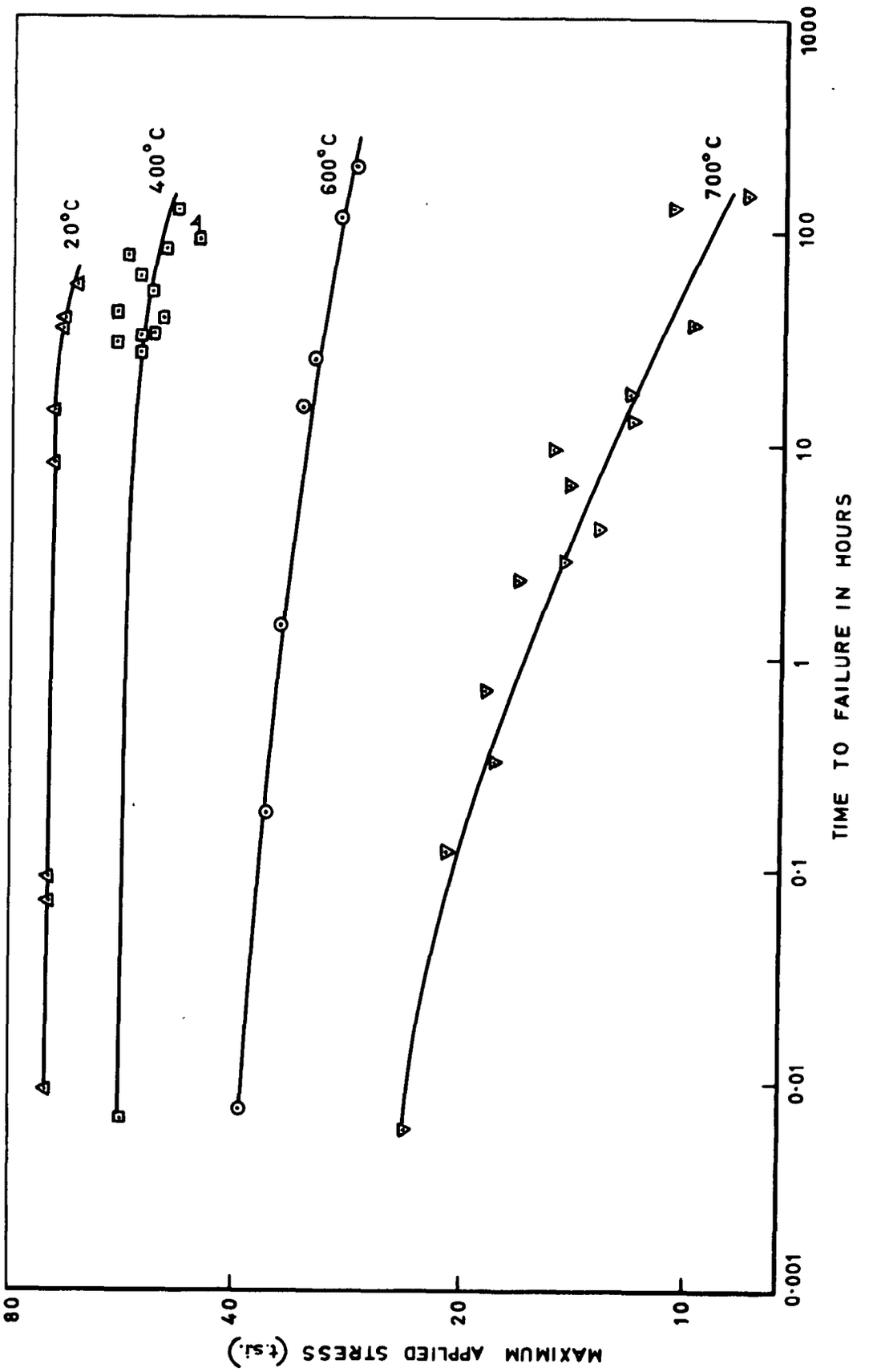

REPEATED TENSION
STRESS/TIME FATIGUE RUPTURE CURVES
AT 6C/M

FIG.4

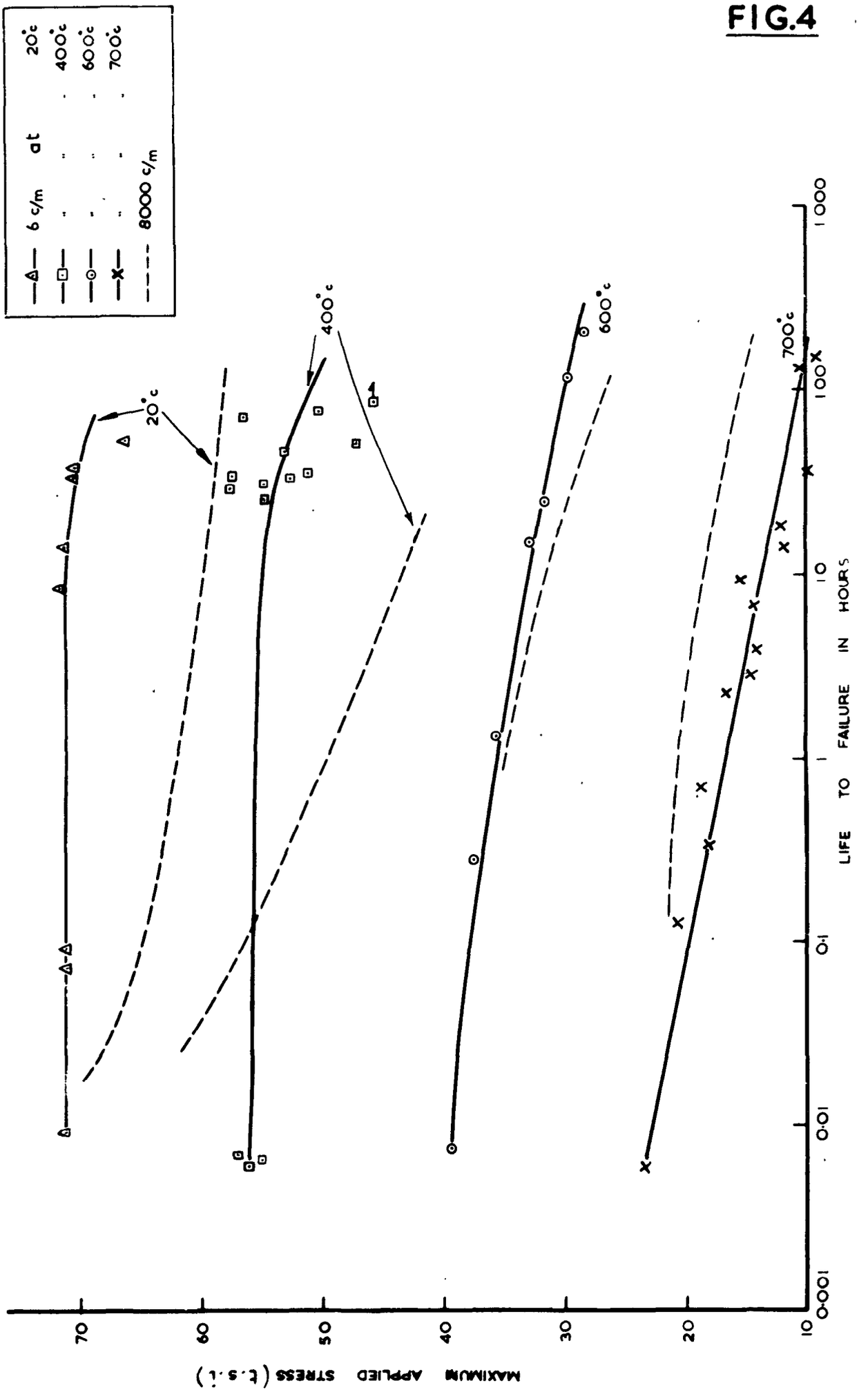

REPEATED TENSION STRESS / TIME RUPTURE CURVES AT 8000 C/M & 6C/M.

FIG.5.

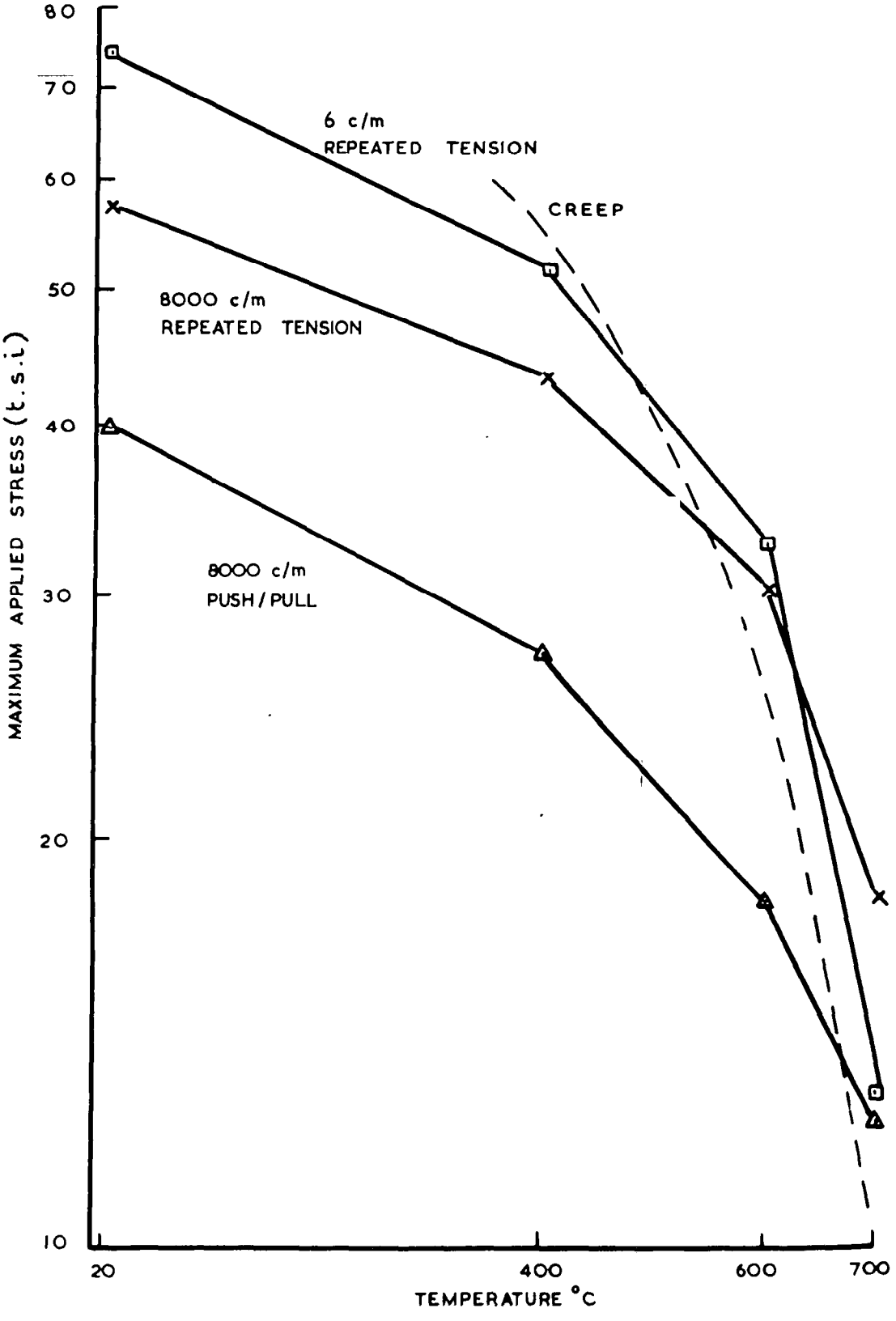

STRESS/TEMPERATURE FATIGUE & CREEP 10 HR. CROSS-PLOTS

FIG. 6

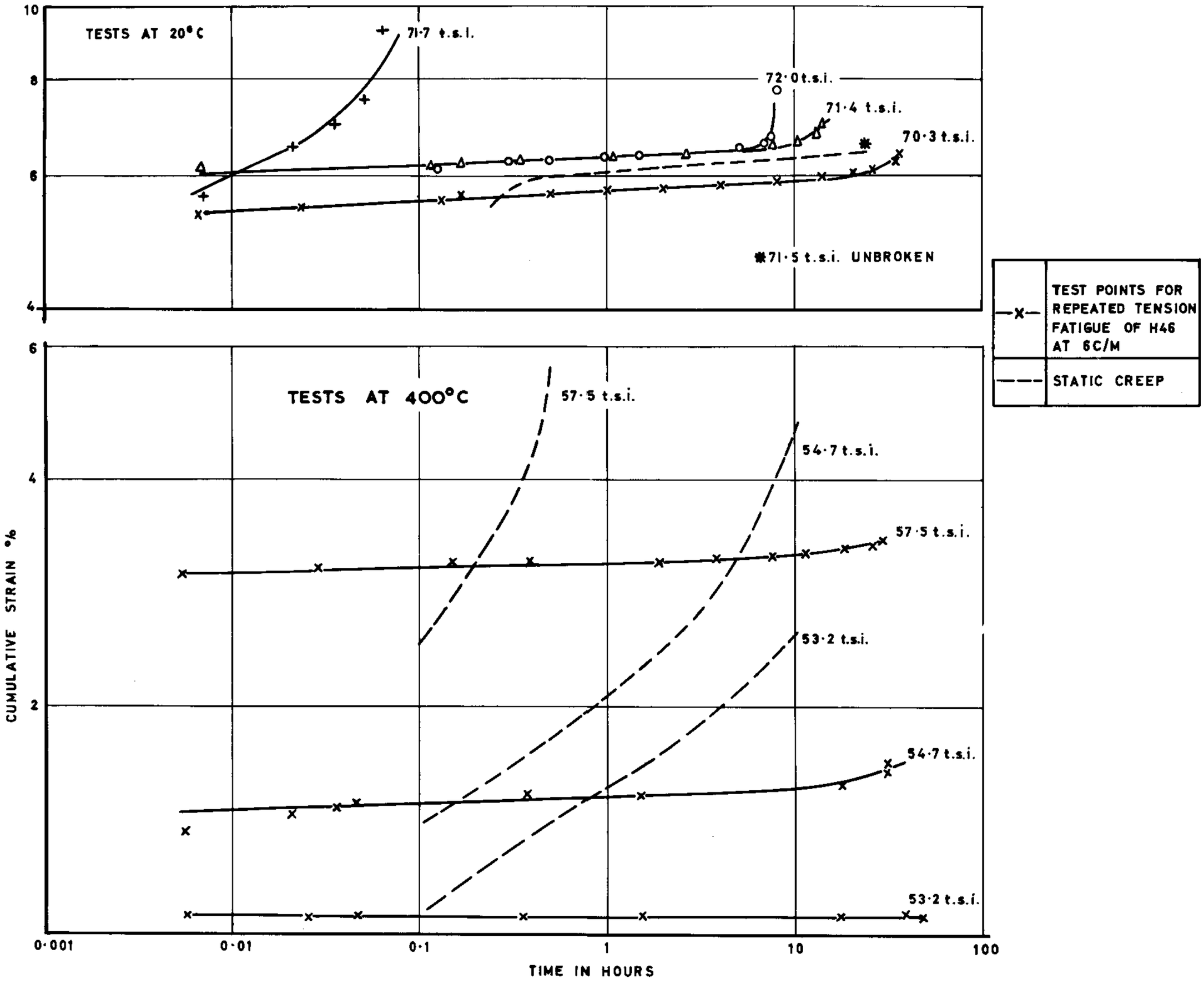

CUMULATIVE STRAIN/TIME CURVES AT 20°C AND 400°C.

FIG. 7

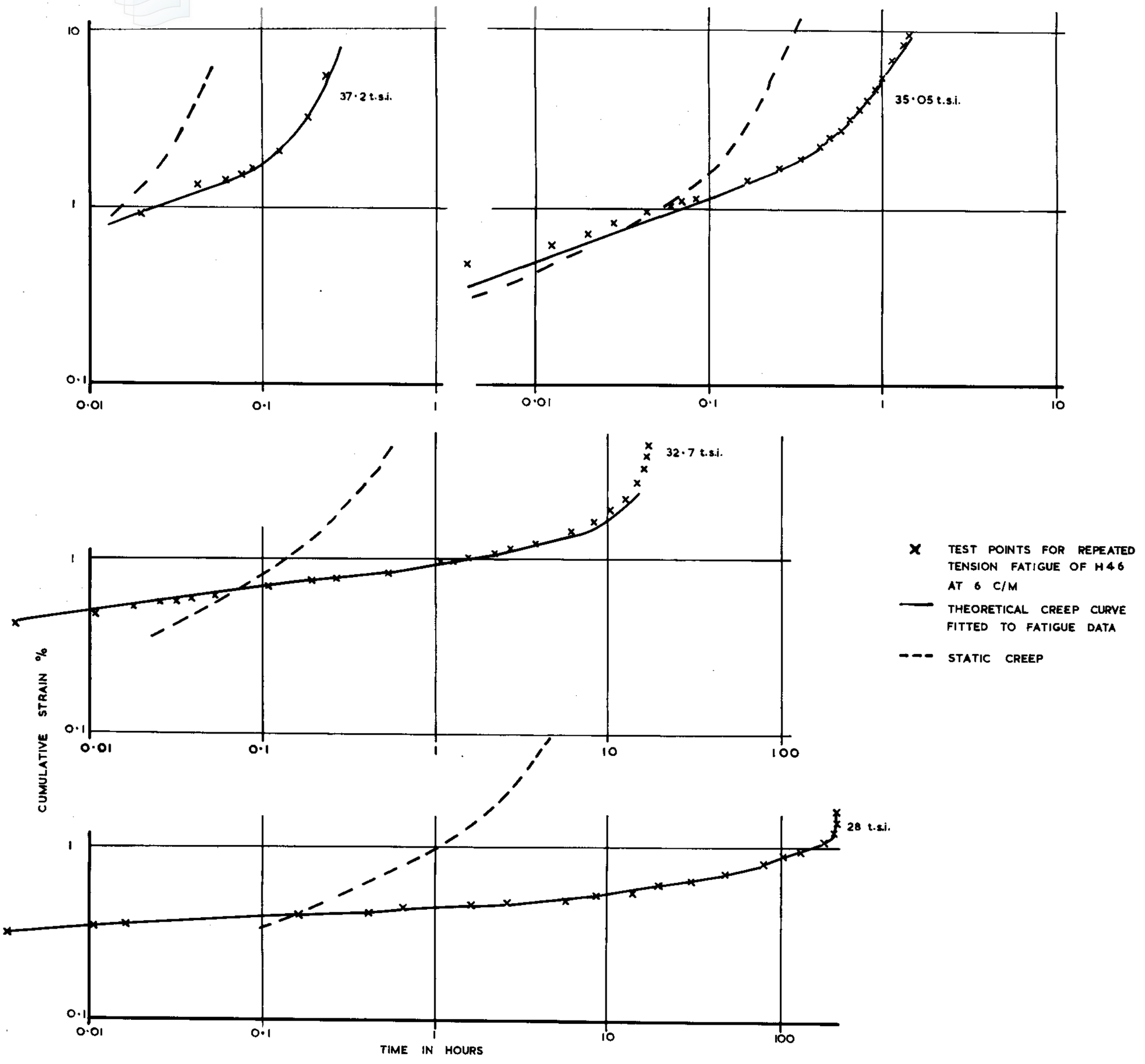

CUMULATIVE STRAIN / TIME CURVES AT 600°C.

FIG.8

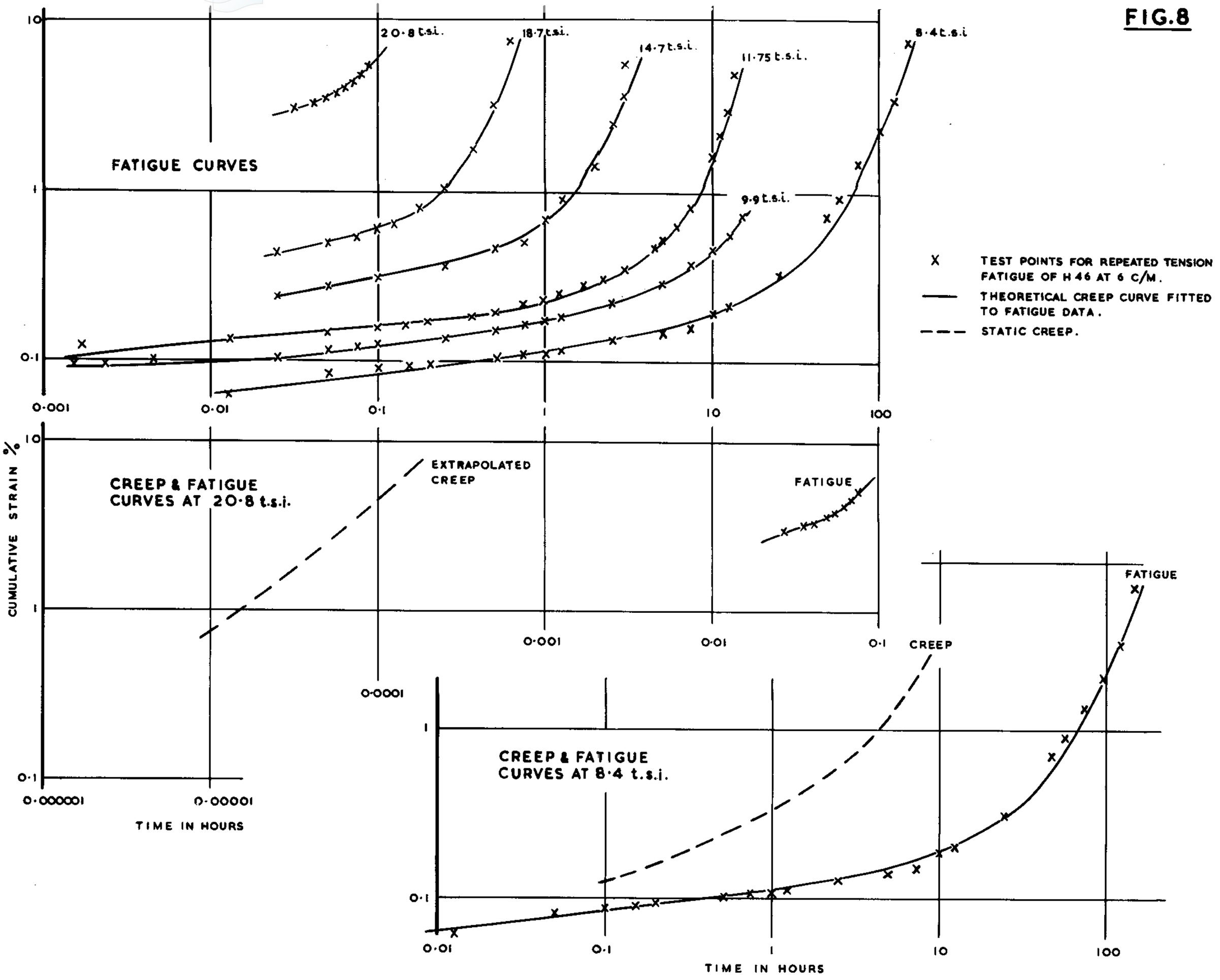

CUMULATIVE STRAIN/TIME CURVES AT 700°C

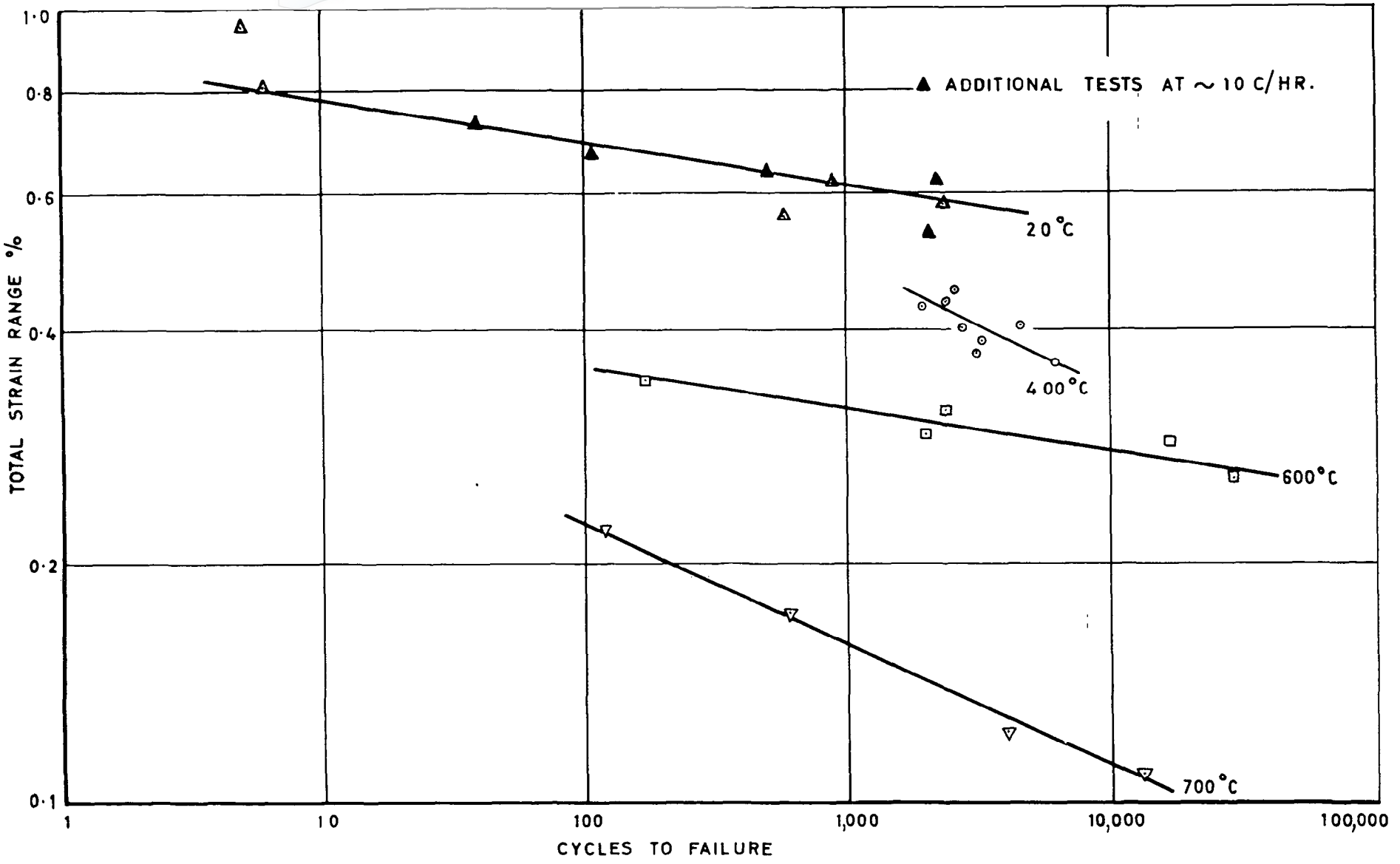

TOTAL STRAIN RANGE/CYCLES TO FAILURE CURVES FOR REPEATED TENSION AT 6 C/M

FIG.9

FIG. 10

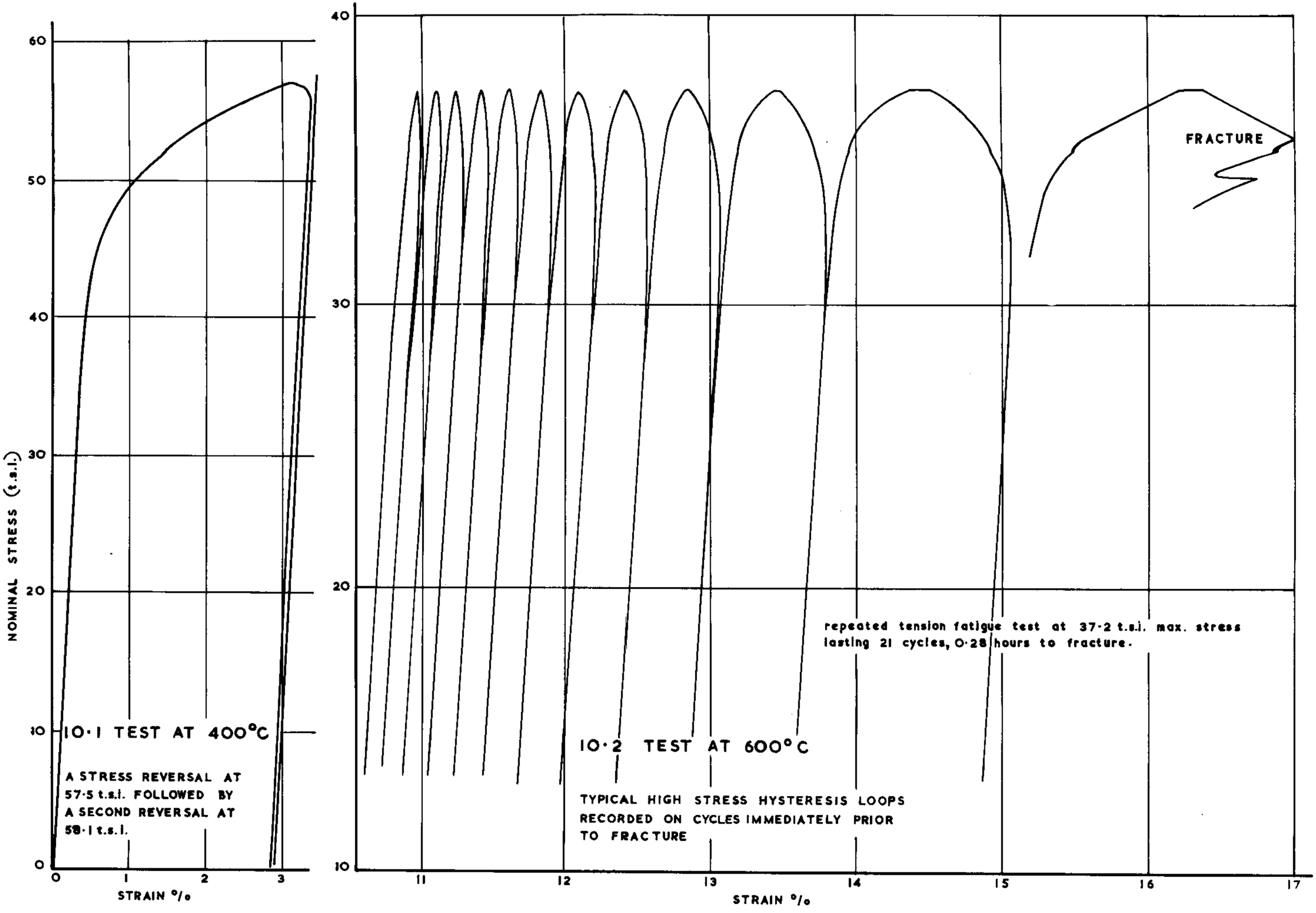

CYCLIC STRESS / STRAIN CURVES AT 400°C AND 600° C.

A.R.C. C.P. No. 788
June, 1964
Tilly, G. P.

539.431:536.49:
669.15-194.57

EFFECTS OF VARIED LOADING PATHS ON FATIGUE ENDURANCES
PART III - SOME STRESS FATIGUE PROPERTIES OF
H46 AT ELEVATED TEMPERATURES

Constant stress amplitude fatigue tests have been carried out on an 11 per cent Cr-Mo-V-Nb steel (H46). The tests were conducted at 20°C, 400°C, 600°C and 700°C at 8000 c/m for push/pull and repeated tension loading, and at 6 c/m for repeated tension and were compared with available creep data of the same H46 forging. The resistance to static creep was greater than that to fatigue at 20°C and 400°C, but was less at 700°C. Similarly, the resistance to repeated tension fatigue at 8000 c/m was greater than that to 6 c/m fatigue at 700°C, but was less at 20°C.

P.T.O.

A.R.C. C.P. No. 788
June, 1964
Tilly, G. P.

539.431:536.49:
669.15-194.57

EFFECTS OF VARIED LOADING PATHS ON FATIGUE ENDURANCES
PART III - SOME STRESS FATIGUE PROPERTIES OF
H46 AT ELEVATED TEMPERATURES

Constant stress amplitude fatigue tests have been carried out on an 11 per cent Cr-Mo-V-Nb steel (H46). The tests were conducted at 20°C, 400°C, 600°C and 700°C at 8000 c/m for push/pull and repeated tension loading, and at 6 c/m for repeated tension and were compared with available creep data of the same H46 forging. The resistance to static creep was greater than that to fatigue at 20°C and 400°C, but was less at 700°C. Similarly, the resistance to repeated tension fatigue at 8000 c/m was greater than that to 6 c/m fatigue at 700°C, but was less at 20°C.

P.T.O.

A.R.C. C.P. No. 788
June, 1964
Tilly, G. P.

539.431:536.49:
669.15-194.57

EFFECTS OF VARIED LOADING PATHS ON FATIGUE ENDURANCES
PART III - SOME STRESS FATIGUE PROPERTIES OF
H46 AT ELEVATED TEMPERATURES

Constant stress amplitude fatigue tests have been carried out on an 11 per cent Cr-Mo-V-Nb steel (H46). The tests were conducted at 20°C, 400°C, 600°C and 700°C at 8000 c/m for push/pull and repeated tension loading, and at 6 c/m for repeated tension and were compared with available creep data of the same H46 forging. The resistance to static creep was greater than that to fatigue at 20°C and 400°C, but was less at 700°C. Similarly, the resistance to repeated tension fatigue at 8000 c/m was greater than that to 6 c/m fatigue at 700°C, but was less at 20°C.

P.T.O.

Fatigue strain accumulated during the 6 c/m repeated tension tests according to laws similar to those that describe static creep strain behaviour. This was true at temperatures as low as 20°C provided the applied stresses were high enough. Static creep strain accumulated at a faster rate than fatigue strain at temperatures of 400°C and above. These differences were enhanced by an increase in temperature or stress.

The total secondary fatigue strain range (ε_T) appeared to be related to the number of cycles to failure (N) by an expression of the form $\varepsilon_T N^{\alpha}$ which was constant for a given temperature. The values of the exponent α varied according to the temperature.

Fatigue strain accumulated during the 6 c/m repeated tension tests according to laws similar to those that describe static creep strain behaviour. This was true at temperatures as low as 20°C provided the applied stresses were high enough. Static creep strain accumulated at a faster rate than fatigue strain at temperatures of 400°C and above. These differences were enhanced by an increase in temperature or stress.

The total secondary fatigue strain (ε_T) appeared to be related to the number of cycles to failure (N) by an expression of the form $\varepsilon_T N^{\alpha}$ which was constant for a given temperature. The values of the exponent α varied according to the temperature.

Printed and published by
HER MAJESTY'S STATIONERY OFFICE

To be purchased from
York House, Kingsway, London W.C.2
423 Oxford Street, London W.1
13A Castle Street, Edinburgh 2
109 St. Mary Street, Cardiff
39 King Street, Manchester 2
50 Fairfax Street, Bristol 1
35 Smallbrook, Ringway, Birmingham 5
80 Chichester Street, Belfast 1
or through any bookseller

Printed in England

C.P. No. 788

S.O. Code No. 23-9015-88